Infiltration capacity of cracked pavements

31th May 2018, Revised version of manuscript first submitted 20 December 2017

Charlotte Salt BEng
Department of Architecture and Civil Engineering, University of Bath, Bath, BA2 7AY, United Kingdom

Glanville Consultants, Didcot, United Kingdom

*Thomas R Kjeldsen MSc PhD
Department of Architecture and Civil Engineering, University of Bath, Bath, BA2 7AY, United Kingdom
ORCID number: 0000-0001-9423-5203

***Corresponding author.**

5456 words
Number of figures: 8
Number of tables: 3

Abstract

Understanding the hydrological behaviour of urban surfaces is imperative in the design of surface water drainage systems and flood mitigation strategies, as well as for the modelling of groundwater recharge and pollution. This study has examined the hydrological behaviour of cracked impervious surfaces through field infiltration testing and image analysis of the cracks themselves. Infiltration tests were undertaken on a section of concrete slab pavers paving. Our results showed that cracks in impervious surfaces allow significant volumes of water to infiltrate through them, with infiltration rates comparable to those found in sands and gravels. Using a regression model, infiltration rates were related directly to crack characteristics obtained from image processing software, thereby enabling the first published quantitative link between percentage cracked area and infiltration capacity. The implications of accounting for this infiltration for surface water management systems are estimated to be in the order of £20 million annually for the construction industry in England.

Keywords

Drainage & irrigation; Hydrology & water resource; Roads & highways

List of notation

A_C	is the overall crack area
A_{CATCH}	is the catchment area
A_I	is the inner cylinder area
A_P	is the total pavement area
d	is the water level
D	is the storm duration
D_{VOL}	is the critical storm duration
i	is the indicator variable
IR	is the infiltration rate
p	is the rainfall intensity
PAC	is the percentage area cracked
$QBAR_{RURAL}$	is the greenfield runoff rate
t	is the time taken
V	is the runoff volume
V_D	is the outflow volume
V_S	is the storage volume required
W	is the average crack width

1. Introduction

As cities continue to grow and urban flooding becomes increasingly problematic, improving the understanding of the hydrology of urban man-made surfaces is an important component in the design of effective flood mitigation measures (Arnbjerg-Nielsen *et al.*, 2013). Traditionally, rainfall-runoff models used for design flood prediction in urban catchments are based on simplified assumptions regarding the hydrological behaviour of urban and seemingly impervious areas, for example, assuming fixed runoff rates in the range 70% to 100% (e.g. Kjeldsen, 2009), but without specific reference to the condition of the urban surfaces. However, in a review of published experimental results related to the hydrological performance of common urban surfaces such as roads, roofs, and pavements, Redfern *et al.* (2016) found that observed runoff rates are frequently lower than those adopted in the existing rainfall-runoff models. This effect was attributed to the existence of preferential pathways caused by cracks and joints, typically found in aging infrastructure. A similar conclusion was reached by Davidsen et al. (2017) based on continuous simulation of historical rainfall time series using an urban rainfall-runoff model.

A number of experimental studies have attempted to quantify the infiltration through impervious urban surfaces. Ragab *et al.* (2003) focussed on the proportion of rainfall converted to runoff, infiltration and evaporation and undertook testing at five locations in Wallingford, UK, four of which were existing road surfaces of a variety of ages and one of which was a grass site. Soil moisture content was compared to measured groundwater levels in order to evaluate the amount of rainfall infiltrating through the surfaces over a period of twelve months. The study concluded that soil moisture beneath impervious surfaces increased in response to rainfall. It also found that the ratio of runoff to rainfall varied with the seasons, and that infiltration accounted for between 6 to 9% of total annual rainfall.

Wiles and Sharp (2008) investigated in particular the role of fractures in providing a preferential pathway allowing rainwater to flow through impervious road surfaces. *In-situ* infiltration testing was undertaken on cracked road surfaces in Austin, Texas, USA, and it was found that cracks had a hydraulic conductivity comparable to that of fine-grained sands, sandstones, silts and loams. It was concluded that cracks in the surfaces tested increased infiltration rates, although a correlation between the hydraulic conductivity and crack width was not found. Taylor (2004) undertook infiltration tests on seven sites on the University of Nottingham campus, UK, to investigate the migration of contaminants through pavements. Six of the test sites exhibited either area (e.g. alligator-type) or longitudinal cracking, and one was located on an intact pavement above a service trench. A range of infiltration rates were recorded across the seven sites and were found to be comparable to those found in sandy soils (CIRIA, 1996). However, the study did not directly relate these rates to the crack characteristics.

In contrast to experimental studies, detailed hydrodynamic models have been proposed by Chen *et al.* (2004), Hou and Luo (2013) and Dan *et al.* (2016) directly relating infiltration to crack characteristics. Both Chen *et al.* (2004) and Dan *et al.* (2016) determined that a quadratic relationship exists between crack width and infiltration rates, however Hou and Luo (2013) found that the width of the crack, whilst increasing flow rates, had less influence than other factors. These theoretical studies did not validate their models against experimental data.

Although it is commonly accepted that cracks increase infiltration rates (e.g. Hollis, 1988, and supported by the scientific evidence summarised above), a relationship between crack characteristics and infiltration rates has yet to be proven experimentally; previous experimental studies investigating infiltration through urban surfaces have either not recorded crack characteristics (e.g. Taylor, 2004), or have relied upon manual measurements (e.g. Wiles and Sharp, 2008).

In order to develop the findings of experimental studies into a more generic modelling system which represents the hydrological response of urban surfaces where no runoff data exists, it is necessary to predict infiltration rates based on crack characteristics that can be easily obtained from field studies. In order to address this aim, a method of computerised image processing was developed as part of this study. This provided a more accurate and efficient method of determining crack characteristics such as width and length, as well being able to determine overall crack area. This information was used to derive the percentage of impervious surface which exhibited cracking, the percentage area cracked. Specifically, the aim of this study is to investigate the rate of infiltration through cracks in a pedestrian pavement and to relate the infiltration rate to easily derived crack characteristics visible from images, such as crack area and width, and overall percentage area cracked. This will enable a new predictive model of infiltration rates through cracked pavements to be developed, which will in turn lead to an improved understanding of the hydrological behaviour of impervious surfaces and therefore potential cost savings to the construction industry.

2. Methodology

2.1 Infiltration measurement

In this study infiltration is defined as the rate (mm/hour) at which water flows through a crack in a pavement and into the underlying strata. Different experimental procedures for measuring infiltration have been proposed in the literature, including constant head tests (e.g. Taylor, 2004) and falling head tests (e.g. Bean, 2005; Wiles and Sharp, 2008). A falling head test was adopted for this study as it was considered by Wiles and Sharp (2008) to work well for both high and low infiltration rates and to take less time than a constant head test. Bean (2005) also noted that this method reduced water usage.

The methodology followed in this study used a double-ring infiltrometer consisting of an inner and outer cylinder, similar to the set-up used in the ASTM C1701 Method for pervious concrete (ASTM International, 2009). The purpose of the outer cylinder was to reduce any horizontal flow through the pavement and cracks which extend beyond the test cylinder, as described by Bean (2005) and Wiles and Sharp (2008). This experimental set-up is shown in Figure 1 and Figure 2. Both cylinders were filled with water and water depth measurements taken within the inner cylinder using digital callipers at intervals of between one and two minutes, or longer where draining of the cylinder was slow. The water in the outer cylinder was topped up throughout the test to maintain a constant depth (head) and therefore flow. The duration of each test was two hours, or until all of the water had drained out of the inner cylinder, whichever occurred first. Recorded water levels were plotted as a function of time for each test; an example of the test data is shown in Figure 3.

FIGURE 1

FIGURE 2

FIGURE 3

Infiltration rates (IRs) were initially determined using three different methods. Method 1 involved fitting a linear regression line to the water level-time profile using the ordinary least square estimation technique, as shown in Figure 3. The fitted linear of the model for the test shown in Figure 3 is of the form:

$$d = -15.77\ t + 40.03 \qquad [1]$$

where *d* is the water depth (mm) and *t* is the time taken (hour).

The absolute value of the slope of this line was taken from equation [1] and used as the IR, similar to Bean (2005). For the regression line reported in equation [1], the IR is thus estimated to be 15.77 mm/hour.

Method 2 involved calculating the total change in water level observed during the test and dividing by the total time taken, as shown in equation [2].

$$IR = \frac{\Delta d}{\Delta t} \qquad [2]$$

For the data in Figure 3 the IR was estimated using Method 2 to be 15.49 mm/hour.

Method 3 was based on the Building Research Establishment (BRE) Digest 365: Soakaway Design method (BRE, 2016). First, a second-order polynomial regression line was fitted to the water level-time profile, as shown in Figure 3. The time elapsed at 75% and 25% of the initial water depth was determined using the equation of this line (equation [3] for Figure 3) and the IR calculated using equation [2].

$$d = 1.20\, t^2 - 18.12\, t + 40.73 \qquad [3]$$

For the data in Figure 3, the IR was calculated using Method 3 to be 15.05 mm/hour.

For some datasets the recorded drop in water level was less than 25% of the total water depth, and in such cases Method 3 involved extrapolation of the water level-time graph in order to find the 75% and 25% water depths. This lead to a higher risk of introducing errors. In addition, for some tests where the data needed to be extrapolated, the second-order polynomial regression line plotted did not produce time values for the water depths required, which lead to this method of calculation only being suitable for half of the tests. In contrast, methods 1 and 2 were able to be applied to all datasets. Method 2 was chosen to be used in the analysis of results as it was applicable to all of the datasets and provided a reliable, simple and consistent approach. It is worth noting that all three methods resulted in relatively similar infiltration rates across all tests.

2.2 Characterising pavement cracks

Developing a predictive model of infiltration rates requires the development of a set of crack characteristics that can be used for describing each individual crack and extracted relatively easily. Rather than relying on manual measurements, a method of computerised image processing was developed, providing a more accurate and consistent method of determining crack characteristics, specifically: crack area (A_C), width (W) and length (L), as well as percentage area cracked (*PAC*). The open-source Image processing software *ImageJ* (Schneider *et al.*, 2012; Schindelin *et al*., 2012) was used to analyse images of the tested pavement surfaces and extract the characteristics.

The image processing sequence developed was as follows:

- Import image of tested pavement (including crack) into the *ImageJ* software.
- Convert image scale from pixels to *mm* by scaling to a known distance on the image.

- Crop image to the size of the inner cylinder to represent the tested area.
- If required, manually adjust the image to “remove” soil or vegetation in the crack or surrounding pavement which could result in a lower contrast between the two; a lower contrast was found to result in difficulty in determining the true crack extents.
- Adjust the colour intensity threshold such that areas of lower intensity (the crack) are converted to white pixels.
- Use the software to calculate the number of white pixels, and therefore calculate the total crack area, A_C.
- Draw along the centreline of the crack using the segmented line tool and use the software to calculate the length of the line representing the crack (L).
- Determine the average crack width, W:

$$W = \frac{A_C}{L} \quad [4]$$

- Determine the percentage area cracked, PAC:

$$PAC = \frac{A_C}{A_I} \quad [5]$$

where A_I is the inner cylinder area.

The crack characteristics obtained from the *ImageJ* processing method were validated against manual measurements of crack width and length, and it was concluded that the *ImageJ* method gave a more accurate representation of actual crack characteristics. This was largely due to only five manual measurements of crack width being taken along the length of each crack, when the actual crack width varied in between each measurement; the average of these measurements taken therefore did not necessarily accurately represent the average crack width. In addition, the manual measurement of the crack length was taken as a direct line between the ends of the crack, when in reality the cracks changed direction along their length; *ImageJ* could account for these changes in direction. It was therefore anticipated that *ImageJ* measured lengths would be longer than the measured lengths, which was found to be the case in all tests.

3. Case study

A total of eight distinct infiltration tests were undertaken on a section of concrete slab pavers on the University of Bath campus, along the northern boundary of South (A) car-park, as detailed in Table 1.

TABLE 1

Each test was conducted as described in Section 2 and each IR estimated using Method 2, while Methods 1 and 3 were used to check that the results were consistent and reasonable.

Soakage tests had previously been carried out by others less than 100m from the section of pavement tested, within soils understood to be of similar conditions to that underlying the pavement tested. Infiltration rates were calculated using Method 3, at between 2081 mm/hr and 2765 mm/hr (Mann Williams, 2016), within the range exhibited by gravels (CIRIA, 1996).

3.1 Uncontrollable factors

The tests in this study were conducted on existing pavement slabs, and thus an intrusive test was considered impractical. As such, there were a number of factors which are considered to potentially effect the infiltration through pavement surfaces which were unfeasible to control or measure. Dan *et al.* (2016) concluded that the infiltration rate is dependent on the pavement layer permeability and thicknesses, and Hou and Luo (2013) also concluded that the permeability of asphalt caps was influenced by the permeability of sediment which had built up within cracks. Infiltration through pavements is also considered to be affected by the properties of the soil underlying the surface (Redfern *et al.*, 2016). These factors were impractical to measure in this study without doing intrusive testing, however, given that the test sites were located on the same section of pavement, it was anticipated that both the underlying geology and lower layers of the pavement structure at each test location were relatively similar. It is also acknowledged that the damage within the pavement structure may differ from that exhibited on the surface, especially in older constructions, and that this may influence the infiltration rate (Taylor, 2004). This is a factor which would have been impractical to measure and this study has focussed on whether a relationship can be established between the damage exhibited on the surface and the infiltration rate. Finally, pavements with shallow gradients were selected, as sloping ground could influence the infiltration measurements by introducing a differential head within the test cylinder.

All tests were undertaken within a five-week period in February and March 2017 (see Table 1). Infiltration can also depend on seasonal variations, with freeze-thaw weathering opening cracks and pore spaces within the surface course and potentially increasing the infiltration rate in winter months (Taylor, 2004). It should be noted that temperatures were above freezing for all tests undertaken. Finally, as recommended by Bean (2005), no infiltration testing occurred within 24 hours of measurable rainfall. This enabled each test to be undertaken under similar antecedent pavement and soil saturation conditions.

4. Results

Table 2 shows the infiltration rate (IR), crack area (A_C), width (W), length (L) and percentage area cracked (PAC) for each of the locations tested, alongside images of the cracked pavement itself. The rates calculated are comparable to those exhibited by sands, and the low end of gravels (CIRIA, 1996) and are also within the ranges found in previous road surface infiltration studies, namely Taylor (2004) and Wiles and Sharp (2008).

TABLE 2

The infiltration rates calculated were plotted against crack area, width and percentage area cracked for each test, as shown in Figure 4, Figure 5 and Figure 6 respectively. Due to the limited number of data points, linear least squares regression lines were considered most appropriate and were fitted through the data points in each figure. An intact slab is considered to completely prevent infiltration through its surface and therefore the y-intercepts for the regression lines were set to zero in order to represent this, thereby reducing the complexity of the model to a single parameter; the slope of the lines.

FIGURE 4

FIGURE 5

FIGURE 6

Inspection of Figures 4, 5 and 6 indicates that Test 8 may represent an outlier, with a higher infiltration rate than expected. As discussed previously, the infiltration through pavement surfaces can be affected by a number of factors which were considered impractical to control and were beyond the scope of this study. It was noted that the slab tested in Test 8 was smoother and lighter in colour than other slabs tested and it is possible that it could have been newer and / or of different construction. It was also observed that the crack contained less sediment than found in other cracks tested. It could also be possible that leakage from the inner test cylinder could have occurred undetected during the test, leading to a higher rate than anticipated.

This aspect was investigated further by fitting linear regression lines through the dataset including and excluding Test 8, and extrapolating these trendlines to find the y-intercept in each case. As mentioned previously, the infiltration rate through an intact slab is expected to be close to or equal to zero, thus the y-intercept of the linear trendlines is also expected to be close to or equal to zero. Inclusion of the Test 8 data point gave y-intercepts of around 10 mm/hour. Removal of Test 8 from the dataset results in values just below 0 mm/hour. It was therefore considered appropriate to remove Test 8 from the data analysis. The linear regression lines plotted on Figures 4, 5 and 6 therefore exclude Test 8.

Figure 4, 5 and 6 indicate that infiltration rates increase as crack area, width and PAC increase and these relationships are summarised in Table 3. The p-values reported in the Table shows that the estimated slope coefficients are significantly different from zero, thus supporting the hypothesis that infiltration rates can be estimated using crack characteristics. This was anticipated as cracks provide a preferential pathway for water ingress into pavements.

TABLE 3

As a similar study has not been attempted before which defines a relationship between these parameters, there is no benchmark to which a comparison can be made. However, given the variability in measurements expected due to uncontrollable factors, the R^2 values reported in Table 3 are considered reasonable for this study, with deviation of data points from these trendlines attributed to the uncontrollable factors already discussed.

Comparison of Figure 4 and Figure 5 shows that the IR-A_C and IR-W relationships are very similar and are therefore both influencing factors on the amount of infiltration, as expected. Their similarity can largely be attributed to the strong correlation between crack width and area. Similarly, the IR- A_C and IR-PAC relationships are correlated due to the method of calculation of PAC.

5. Discussion

Given that the linear regression models without the set intercept at 0 mm/hour gave negative y-intercepts, this suggests that a more curved relationships could potentially be more appropriate, similar to the quadratic relationships proposed by Chen *et al.* (2004) and Dan *et al.* (2016) derived from their theoretical models, where the rate of infiltration rate growth increases after a certain crack width. The results of these studies are plotted approximately on Figure 5, by using the graph given by Chen *et al.* (2004) and the equation given by Dan *et al.* (2016) in their respective studies. From inspection of Figure 5, these models suggest significantly higher rates than those obtained in this study by field experiments. However, these models are not validated against field studies and therefore the disparity noted may be due to the models not accounting for real-life conditions, such as build-up of sediment within cracks, and also only considering infiltration through the crack itself, not the effect of the surrounding impervious pavement.

A comparison of the findings from this study can also be made to the experimental studies of Wiles and Sharp (2008) and Taylor (2004). Infiltration rates calculated in this study are within the ranges of those found in these studies, and are most similar in range to those reported by Taylor (2004). This may be due to similarity in experimental set-up and calculation of infiltration rates, and the tests being undertaken under broadly similar climatic conditions and on pavements of similar construction. This study found a higher average rate than Taylor (2004) and Wiles and Sharp (2008), which could be due to the selection of test locations in this study for their crack characteristics. In particular Wiles and Sharp (2008) tested some joints, which commonly contain some form of sealant, intact pavements, and cracks with narrower widths than tested in this study, which could account for the lower average rates found. Wiles and Sharp (2008) also found some infiltration rates that were significantly higher than those found in this study, which could be due to the fact that some significantly wider cracks were tested than in this study, and also as a result of testing different types of pavements, lack of sediment in the cracks, or the permeability of the underlying soil.

6. Implications for hydrological design

As demonstrated in this study and others, the presence of cracks in impervious surfaces increases the amount of water able to infiltrate through the surface. An assumption commonly made in some hydrological models that 100% of rainfall is converted to runoff on impervious road surfaces (e.g. Warhurst *et al.* 2014) is therefore incorrect, and accounting for this reduction in runoff volume will lead to the development of more realistic rainfall-runoff models. Hydrological models are used in the design of surface water drainage systems, a key component of which are storage structures, which are used to reduce flood risk caused by surface water runoff in new developments. Reducing the volume of runoff assumed from so-called impervious surfaces in hydrological models therefore has the potential to reduce the volume of storage required to attenuate surface water flows in urban areas.

A basic inflow-outflow model has therefore been produced in this study in order to investigate the effect of allowing for infiltration through impervious pavement surfaces on the volume of storage required within a surface water drainage system. In this model it has been assumed that cracks in impervious road surfaces behave in similar way to cracks in impervious pavement surfaces.

6.1 Method

Rainfall depths for a catchment in Bath, UK have been calculated based on the Flood Studies Report (FSR) design rainfall model (NERC, 1975). An arbitrary road catchment area of 1000m^2 was used to represents the total area of impermeable road surfacing within a development. Rainfall depths, *R*, were calculated using a return period of 100 years, with no allowance for climate change, for storm durations (*D*) of 10, 15, 30, 60, 120, 240, 360, 600, 1440 and 2880 minutes. The 100 year return period was chosen as it is the typical design storm used in industry to size surface water storage (Environment Agency, 2013). A simplifying assumption that rainfall was constant throughout each storm duration was made in order to convert each rainfall depth to a rainfall intensity, *p* (mm/hour).

Road surfaces degrade over their lifetime, with the percentage of cracking over the surface increasing over time, thereby increasing the infiltration capacity of the surface. An existing model of road surface degradation proposed by Mubaraki (2014) has been used to determine the PAC for a pavement at yearly intervals between zero (new and intact) and eight years old.

In order to account for losses due to infiltration, the infiltration rate of the pavement was calculated at each yearly interval using the IR –PAC relationship found in this study (Table 3). The rate was assumed to be constant for each storm duration and as such does not account for pavement or soil saturation during rainfall events. The infiltration rate was subtracted from the rainfall intensity, *p*, for each storm duration in order to determine the impact of this increase in infiltration on the runoff volume, *V*, as:

$$V = \frac{1}{60\,000} A_P \, D \, i(p - IR) \quad [6]$$

where *V* is runoff volume (m^3), A_P is total pavement area (m^2), *D* is the storm duration (minutes) *p* is rainfall intensity (mm/hour), *IR* is infiltration rate (mm/hour), indicator variable *i* is one if precipitation exceed infiltration ($p > IR$) and zero otherwise, and 60,000 provides the unit conversion.

The percentage reduction in V from the original value for the initially intact road surface was plotted in Figure 7 against pavement age for the critical volumetric storm duration for each year.

FIGURE 7

The critical volumetric storm duration, D_{VOL}, is defined in this study as that which produces the largest value of V, which was different for different road ages. Figure 7 shows that there is a significant reduction in runoff volume associated with an increase in road cracking of around 40% in the first year of a pavement's life.

6.2 Results

The impact of this reduction in runoff volume on the volume of storage required to attenuate surface water on a development site was assessed by first defining an outflow rate from the catchment. A constant discharge rate equal to the mean annual maximum flood representing greenfield runoff rate, $QBAR_{RURAL}$, for the catchment area was considered appropriate to use for this simple model. $QBAR_{RURAL}$ was calculated using the IH 124 method (Institute of Hydrology, 1994):

$$QBAR_{RURAL} = 0.00108 \times (0.01 \times A_{CATCH})^{0.89} \times SAAR^{1.17} \times SPR^{2.17} \qquad [7]$$

where $QBAR_{RURAL}$ is greenfield runoff rate (m^3/s), A_{CATCH} is the catchment area (hectares), $SAAR$ is standard annual average rainfall (mm) and SPR is standard percentage runoff. As the catchment area in this model is under 50 hectares, the IH 124 method was applied with 50 hectares in the formula and linearly interpolated using the ratio of the catchment area to 50 hectares (National SUDS Working Group, 2004). A $SAAR$ value of 819 mm and SPR value of 0.37 were used in this model, representing conditions found in the geographical vicinity of where the field data was obtained in this study.

The total outflow volume, V_D, from the storage structure calculated as follows:

$$V_D = D\ QBAR_{RURAL} \quad [8]$$

The preliminary sizing of a surface water storage structure can be derived by using the difference between the inflow (runoff volume, *V*) into the storage structure and the outflow (discharge volume, V_D):

$$V_S = V - V_D \quad [9]$$

where V_S is the storage volume required.

The percentage reduction in V_S required from the value for the intact road surface was plotted in Figure 8 against pavement age for D_{VOL} for each year.

FIGURE 8

The results in Figure 8 show that, as for the runoff volume, there is significant reduction in storage volume required of around 40% in the first year of a road's life when considering infiltration through cracks. Note that the values of runoff and storage volumes are directly related as the outflow volume for each storm duration does not change over time; thus Figures 7 and 8 show identical relationships.

6.3 Discussion

This reduction in volume of storage could represent both material and cost savings and a simple calculation has been undertaken to assess this impact. Cost estimates were based on a study by Stovin and Swan (2007), which reported that a standard reinforced concrete storage tank costs between £448.50/m^3 and £518.29/m^3 to construct, leading to cost savings for the catchment area defined in this model of between £5,582 and £6,451 (40% of the original price) if the drainage system were to be designed to a one-year-old road, rather than assumed to be completely intact.

This then allows the cost savings for new housing developments to be assessed on a wider scale. The road catchment area of 1000m^2 used in this model can be assumed to represent the total impervious road area within a housing development of approximately 20 dwellings. In 2016, 140,660 new homes were constructed in England (Department for Communities and Local Government, 2017). A conservative assumption can be made that 50% of these developments are either served by roads of pervious construction, are flats or are single dwellings not requiring access roads. Extrapolating the road catchment area of 1000m^2 per 20 houses, and applying the cost savings made by designing to a one-year-old road, this could represent cost savings to the construction industry of up to £20 million a year. This model could be extended to wider infrastructure, such as trunk roads, and commercial and industrial developments, thereby further increasing the potential cost savings.

By accounting for infiltration through cracks and thereby reducing storage tank sizes, a lower level of flood protection against storm events is provided. Therefore, these runoff models should be used in conjunction with an assessment of the joint probability of design storm events occurring before the pavement has deteriorated to the condition to which the storage structures have been designed to.

7. Conclusions

The aim of this study was to investigate the influence of cracks in impervious surfaces on their hydrological behaviour, using *in-situ* testing and computerised image analysis. The field infiltration tests have shown that cracks in impervious surfaces can allow water to infiltrate through them, with infiltration rates comparable to those found in sands and gravels (CIRIA, 1996).

Relationships between crack characteristics and infiltration rates were developed. As the width and overall surface area of cracks, and thus percentage area cracked, increased, their infiltration capacity also increased, as anticipated. Although a conclusive relationship between these parameters was not established, a general trend was determined from the test data. The lack of definitive trend could be due to the factors which were unable to be controlled or measured during the field tests and which may affect the infiltration capacity of the surface, such as amount and type of sediment within the crack, sub-surface pavement condition and underlying pavement construction and soil conditions. Field tests in which some of these factors could be controlled or measured, such as those incorporating intrusive testing methods, could eliminate the influence of these factors. A larger set of test data would also be beneficial to confirm the trend found in this study, especially in the range width between 0 mm and 2.5 mm, area between 0 mm^2 and 1000 mm^2 and *PAC* between 0% and 0.75%.

The infiltration rate to percentage area cracked relationship established in this study has been used in a simple inflow-outflow model to evaluate the effect of allowing for infiltration through impervious surfaces on hydrological models. This model demonstrated that allowing for this increase in infiltration capacity could lead to a reduction in runoff volume and surface water storage volume of around 40% in the first year of a pavement's life. This reduction in volume of storage required represents significant cost savings to the construction industry when designing surface water storage structures for major development and infrastructure projects, or retrofitting SuDS to existing systems. Based on several assumptions, this simple model has demonstrated that accounting for a greater proportion of rainfall being converted to infiltration on road surfaces which have previously been assumed to be impervious could lead to considerable cost savings for the construction industry in England, estimated here to be in the order of £20 million annually.

Repeating the computerised process for each image was feasible for the relatively modest number of images analysed in this study. However, in order to repeat on a larger scale an automated method of crack detection and characterisation would be advantageous. Using field testing alongside improved image analysis techniques could help to develop a model of the amount infiltration through an impervious surface over its lifetime. Using this model in conjunction with an assessment of the joint probability of design storm events and pavement deterioration could then aid in the development of more realistic rainfall-runoff models, which in turn leads to an improvement in surface water drainage system design. It could also be used in the development of computer software which could automatically analyse images of pavements and calculate the proportion of rainfall which will infiltrate, which could then be used to develop local runoff models.

References

Arnbjerg-Nielsen, K., Willems, P., Olsson, J., Beecham, S., Pathirana, A., Gregersen, I.B., Madsen, H. and Nguyen, V.T.V., (2013). Impacts of climate change on rainfall extremes and urban drainage systems: a review. *Water Science and Technology*, 68(1), pp.16-28.

ASTM International (2009). ASTM C1701 / C1701M-09, Standard Test Method for Infiltration Rate of In Place Pervious Concrete. West Conshohocken, PA.

Bean, E.Z. (2005). A field study to evaluate permeable pavement surface infiltration rates, runoff quantity, runoff quality, and exfiltrate quality, M.S. thesis, Department. Biological and Agricultural Engineering, North Carolina State University, Raleigh, NC.

Building Research Establishment (2016). BRE Digest 365: Soakaway Design. London: BRE Bookshop.

Chen, J.-S., Lin, K.-Y. and Young, S.-Y. (2004). Effects of crack width and permeability on moisture-induced damage of pavements. *Journal of Materials in Civil Engineering*, 16(3), pp. 276-282.

CIRIA (1996). Infiltration drainage - manual for good practice (R156), CIRIA, London.

Dan, H.-C., Tan, J.-W., Zhang, Z. and He, L.-H. (2016). Modelling and estimation of water infiltration into cracked asphalt pavement. *Road Materials and Pavement Design*, 18(3) pp. 590-611.

Davidsen, S., Löwe, R., Ravn, N.H., Jensen, L.N. and Arnbjerg-Nielsen, K. (2017) Initial conditions of urban permeable surfaces in rainfall-runoff models using Horton's infiltration. *Water Science and Technology*, p.wst2017580.

Department for Communities and Local Government (2017). House building; new build dwellings, England: December Quarter 2016.

Environment Agency (2013). Rainfall runoff management for developments: Report SC030219, Environment Agency, Bristol,

Hollis, G. E. (1988) Rain, roads and runoff: Hydrology of cities. *Geography*, 73(1), 9-18

Hou, D. and Luo, J. (2013). Evaluation of Apparent Permeability and Field Assessment of Aged Asphalt Capping Systems. *Journal of Environmental Engineering*, 139(2), pp. 167-175.

Institute of Hydrology (1994). Report No. 124 - Flood estimation for small catchments.

Kjeldsen, T.R. (2009). Modelling the impact of urbanisation on flood runoff volume. *Proceedings of the ICE-Water Management*, 162(5), pp.329-336.

Mann Williams (2016). University of Bath: The Milner Centre for Evolution – Drainage Strategy 7922RCW_Drainage Strategy, Bath and North East Somerset Council, Bath.

Mubaraki, M. (2014). Third- order polynomial equations of municipal urban low- volume pavement for the most common distress types. *International Journal of Pavement Engineering*, 15(4), pp. 303-308.

National SUDS Working Group (2004). Interim Code of Practice for Sustainable Drainage Systems.

NERC (1975). *Flood Studies Report* (five volumes), London: NERC.

Ragab, R., Rosier, P., Dixon, A., Bromley, J. and Cooper, J.D. (2003). Experimental study of water fluxes in a residential area: 2. Road infiltration, runoff and evaporation. *Hydrological Processes*, 17(12), pp. 2423-2437.

Redfern, T.W., Macdonald, N., Kjeldsen, T.R., Miller, J.D. and Reynard, N. (2016). Current understanding of hydrological processes on common urban surfaces. *Progress in Physical Geography*, 40(5), pp.699-713.

Schneider, C.A., Rasband, W.S. and Eliceiri, K.W. (2012). NIH Image to ImageJ: 25 years of image analysis. *Nature methods*, 9(7), p. 671.

Schindelin, J., Arganda-Carreras, I., Frise, E., Kaynig, V., Longair, M., Pietzsch, T., Preibisch, S., Rueden, C., Saalfeld, S. and Schmid, B. (2012). Fiji: an open-source platform for biological-image analysis. *Nature methods*, 9(7), pp. 676-682.

Stovin, V.R. and Swan, A.D. (2007). Retrofit SuDS - cost estimates and decision-support tools. *Proceedings of the ICE - Water Management*, 160(4), pp. 207-214.

Taylor, J.V. (2004). Migration of contaminants associated with pavement construction, DPhil thesis, School of Civil Engineering, University of Nottingham.

Warhurst, J.R., Parks, K.E., McCulloch, L., Hudson, M.D. (2014). Front gardens to car parks: Changes in garden permeability and effects on flood regulation. *Science of the Total Environment*, 485, pp. 329-339.

Wiles, T.J. and Sharp, J.M. (2008). The secondary permeability of impervious cover. *Environmental & Engineering Geoscience*, 14(4), pp.251-265.

Figure captions

Figure 1. Schematic diagram of the infiltration test set-up
Figure 2. Image of the *in-situ* infiltration test equipment
Figure 3. Infiltration test data example: Test No. 3 – Graph of water level against time
Figure 4. Infiltration rate against crack width
Figure 5. Infiltration rate against crack area
Figure 6. Infiltration rate against percentage area cracked
Figure 7. Reduction in runoff volume due to infiltration through impervious surfaces over the lifetime of the pavement
Figure 8. Reduction in storage volume due to infiltration through impervious surfaces over the lifetime of the pavement

Table captions

Table 1. Details of infiltration tests
Table 2. Crack characteristics summary
Table 3. Summary of regression models linking infiltration rate (IR) to crack characteristics

FIGURE 1

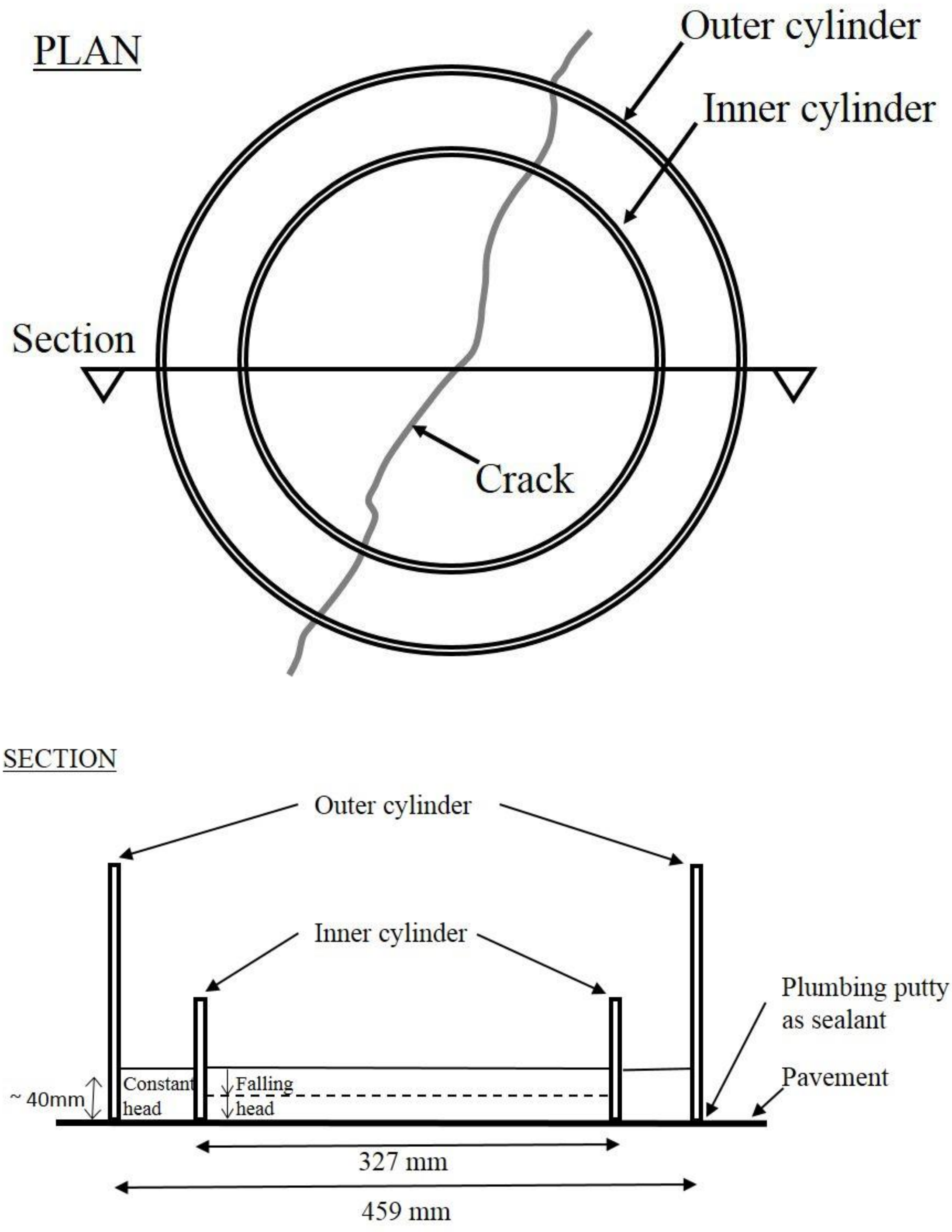
PLAN
Outer cylinder
Inner cylinder
Section
Crack
SECTION
Outer cylinder
Inner cylinder
Plumbing putty
as sealant
Pavement
~ 40mm
Constant
head
Falling
head
327 mm
459 mm

FIGURE 2

FIGURE 3

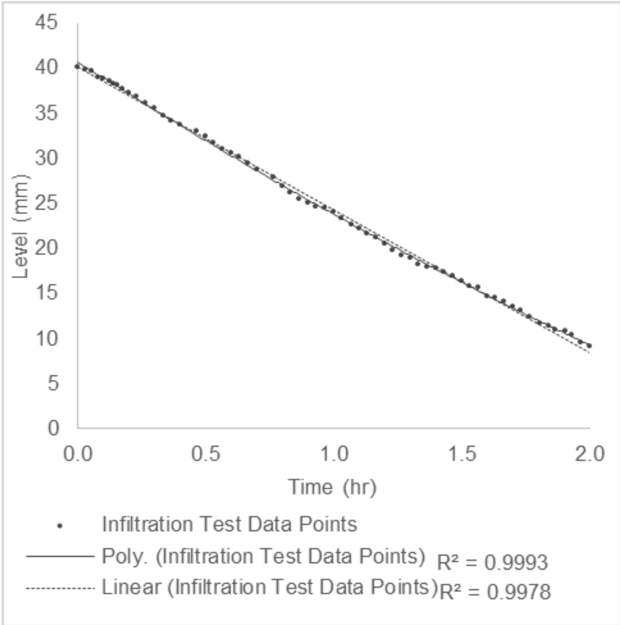
45
40
35
30
25
20
15
10
5
0
Level (mm)
0.0
0.5
1.0
1.5
2.0
Time (hr)
Infiltration Test Data Points
Poly. (Infiltration Test Data Points) R² = 0.9993
Linear (Infiltration Test Data Points) R² = 0.9978

FIGURE 4

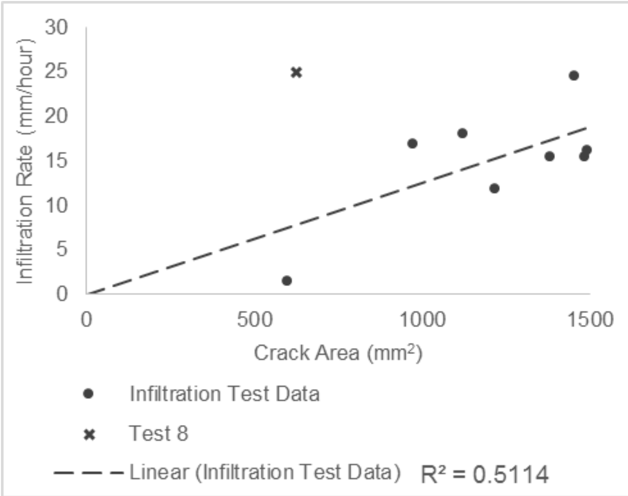
Infiltration Rate (mm/hour)
30
25
20
15
10
5
0
0
500
1000
1500
Crack Area (mm²)
Infiltration Test Data
Test 8
Linear (Infiltration Test Data)
R² = 0.5114

FIGURE 5

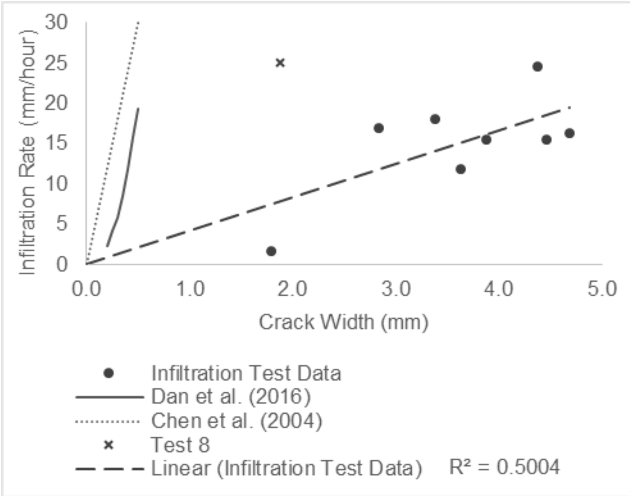
Infiltration Rate (mm/hour)
30
25
20
15
10
5
0
0.0
1.0
2.0
3.0
4.0
5.0
Crack Width (mm)
Infiltration Test Data
Dan et al. (2016)
Chen et al. (2004)
Test 8
Linear (Infiltration Test Data)
R² = 0.5004

FIGURE 6

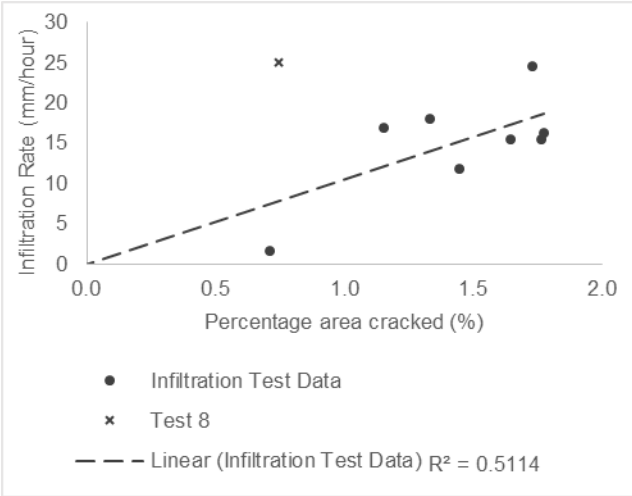
Infiltration Rate (mm/hour)
30
25
20
15
10
5
0
0.0
0.5
1.0
1.5
2.0
Percentage area cracked (%)
Infiltration Test Data
Test 8
Linear (Infiltration Test Data) R² = 0.5114

FIGURE 7

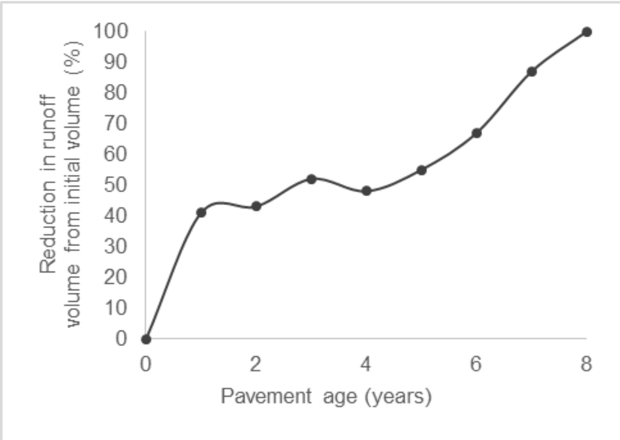
Reduction in runoff volume from initial volume (%)
0
10
20
30
40
50
60
70
80
90
100
0
2
4
6
8
Pavement age (years)

FIGURE 8

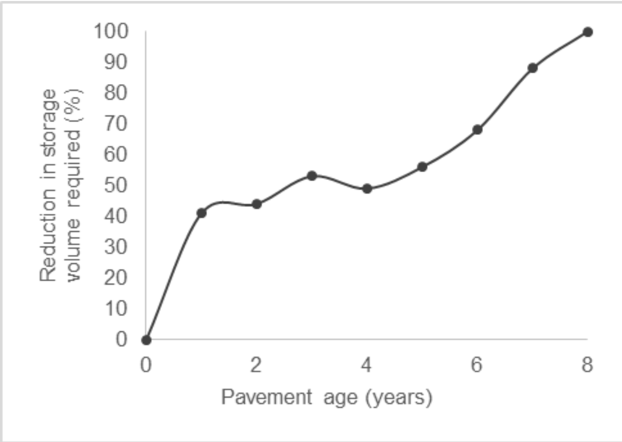
Reduction in storage volume required (%)
100
90
80
70
60
50
40
30
20
10
0
0
2
4
6
8
Pavement age (years)

TABLE 1

Table 1. Details of infiltration tests

Test Number	**ID Number**	**Date DD/MM/YY**	***Notes***
Trial	A	09.02.17	*Trial – 30 minute test*
1	A	17.02.17	*4 No. 30 minute tests*
2	B	19.02.17	*Aborted after pre-wet test*
3	A	24.02.17	
4	C	25.02.17	
5	D	07.03.17	
6	E	10.03.17	
7	F	11.03.17	
8	G	14.03.17	

Table 2: Crack characteristics summary

Test No.	Overall Crack Area (mm2)	Average Crack Width (mm)	Crack Length (mm)	Percentage area cracked (%)	Infiltration Rate (mm/hr)	Crack
Trial	1121.995	3.39	331.352	1.34	18.00	
1	1217.215	3.63	335.294	1.45	11.81	
2	1480.646	4.47	331.519	1.76	15.46	
3	1379.37	3.88	355.525	1.64	15.49	
4	1450.32	4.37	331.761	1.73	24.57	
5	597.726	1.79	334.310	0.71	1.64	
6	1490.292	4.68	318.494	1.77	16.28	
7	970.187	2.84	341.776	1.16	16.98	
8	626.309	1.87	334.102	0.75	25.01	

Table 3. Summary of regression models linking infiltration rate (IR) to crack characteristics

Crack characteristics	**Regression model**	**Range**	**p-value**
Crack area (Ac)	IR = 0.0125 AC	0 < AC< 1000 mm2	< 0.0001
Width (W)	IR = 4.1788 W	0 < W < 2.5 mm	< 0.0001
Percentage area cracked (PAC)	IR = 10.527 PAC	0.75 < PAC < 1.77 %	< 0.0001